Conclusions

The proposed importance of traces of oxidation products in the surfaces of freshly extruded films (and of course fibers) leads to several interesting conclusions. Since surface thermal oxidation can be eliminated by N_2 blanketing, this same approach could be applied to commercial extrusion. However, for high-speed extrusions the cost of blanketing is likely to be prohibitive, especially in view of the fact that the gain in uv stability will probably be only two- or threefold. (Presumably other impurities—unsaturation, Ti residues—become the dominant sources of photoinitiation at very low concentrations of oxidation products.) This same degree of stabilization can also be cheaply realized or exceeded by the compounding of an efficient polypropylene uv stabilizer [0.1–0.5 part per hundred resin (phr)] with the resin.

It is now believed that most efficient uv stabilizers operate by accepting energy from uv-excited chromophores in the polymer (and then harmlessly dissipating this energy) rather than solely by a screening mechanism.[21,22] Such energy-transfer agents must, however, be situated in the immediate vicinity (at least within 50–100 Å) of the excited chromophore for efficient transfer to occur.[23] Since chromophores are concentrated close to the film surfaces, a large fraction of a uniformly distributed uv stabilizer is ineffective,[24] and only additives close to the surface contribute directly to stability. This leads to the possibility of achieving effective uv stabilization by applying a thin surface coating of a stabilizer to a polypropylene film or fiber. Preliminary work indicates that effective stabilization (lifetimes extended *ca.* fivefold) of 22-μ films can be achieved with as little as 0.01 phr of stabilizer which is present as uniform coatings on each surface. This work will be reported in detail in a future publication.

The problem of controlled acceleration of polyolefin degradation during weathering is of current interest in connection with the self-disposal of packaging materials. From Figure 4 it is apparent that a relatively severe pretreatment of polypropylene packaging films by a conventional corona-treatment apparatus (used to improve polymer printability, etc.) might be sufficient to produce a worthwhile acceleration of photodegradation, without sacrificing other essential properties of the films.

Acknowledgments. The authors wish to thank the companies mentioned in the text for supplying polypropylene film samples and releasing processing data.

---

[22] P. J. Briggs and J. F. McKellar, *J. Appl. Polym. Sci.*, **12**, 1825 (1968).

[23] M. Kasha, *Radiat. Res.*, **20**, 55 (1963), and references cited therein.

[24] This ineffective stabilizer may play an important secondary role, such as acting as a reservoir of stabilizer for the surface.

Entanglement in Concentrated Solutions of Polystyrene with Narrow Distributions of Molecular Weight

R. I. Wolkowicz and W. C. Forsman*

School of Chemical Engineering and Laboratory for Research on the Structure of Matter, University of Pennsylvania, Philadelphia, Pennsylvania 19104.

Received April 30, 1970

ABSTRACT: Linear viscoelastic properties were determined for several concentrated solutions of polystyrene with narrow distributions of molecular weight. Measurements were made from the terminal zone to well within the transition zone using a dynamic viscometer of a new design. To interpret the results, we introduced the notion of partial entanglement. For most polymer solutions and melts, a log–log plot of zero-shear-rate viscosity *vs.* molecular weight, M, changes from a straight line segment of slope between 1.0 and 2.0 to one of slope about 3.4 over a relatively narrow range of molecular weights. We defined chain lengths in this molecular weight range as partially entangled; chain lengths below and above this range were considered, in the usual sense, as unentangled and fully entangled. Normal modes of chain motion of index p as defined by Rouse in his theory of viscoelasticity of assemblies of chain molecules correspond to movement of blocks of chain of molecular weights (M/p). This suggests that the various normal modes and their associated relaxation times could also be characterized according to their degrees of entanglement. We then found that Rouse's theory adequately describes the linear viscoelastic behavior of the above polymer solutions when it is modified to include the effects of partial and full entanglement on the longest few relaxation times. Best correlations were obtained by assuming that only odd-order normal modes are affected by entanglement.

Viscoelastic properties of solutions and melts of sufficiently high molecular weight polymers are said to be dominated by the presence of entanglements. The notion that assemblies of long chain-like molecules can form entangled networks has a certain intuitive appeal, especially since it not only explains linear viscoelastic behavior, but non-Newtonian viscosity as well. Nevertheless, it is still true that the concept of chain entanglement has never been placed upon an entirely satisfactory theoretical basis. One of the reasons for this is that there have been few experimental studies of polymer systems with sufficiently narrow distribution of molecular weights. Since most theories have been developed for monodisperse systems, there has been little opportunity to make critical comparisons between theory and experiment. In this paper we present results from a study of the viscoelastic behavior of concentrated solutions of narrow molecular weight distribution polystyrene and interpret our results in terms of molecular theory proposed by Rouse.[1]

We will restrict our deliberations to nonpolar polymer melts and solutions; strong specific intramolecular or intermolecular interactions such as hydrogen bonds could well contribute rheological effects in addition to the entanglement effects of

---

[1] P. E. Rouse, Jr., *J. Chem. Phys.*, **21**, 1272 (1953).

interest here. Furthermore, we are concerned only with solutions sufficiently concentrated that the segments of any chain molecule extensively pervade the domains of their neighbors—that is, solutions that are characterized by a uniform density of polymer segments. For such solutions each segment of any polymer molecule experiences the same hydrodynamic environment, which is an assumption introduced in the development of the theories of interest in this paper. For solutions dilute enough for the polymer molecules to be separated by regions of pure solvent, there is extensive intramolecular hydrodynamic interaction.[2] Such solutions require different theoretical treatment, such as Flory's[3] treatment of intrinsic viscosity, recently placed on somewhat more rigorous ground by Pyun and Fixman,[4] and the Zimm[5] extension of the Rouse theory which is reported to be in good agreement with experiment.[6–11]

Entanglement will be viewed in terms of both steady flow (shear-rate dependent) viscosity and linear viscoelastic behavior. In correlating these two types of behavior, we can adopt a somewhat simplified point of view. It is often adequate to interpret log–log plots of steady zero-shear-rate viscosity η_0 as a function of weight average molecular weight M_w as two straight line segments intersecting at a critical molecular weight M_c.[12] When corrected to constant free volume,[12–14] the low molecular weight segment has a slope of 1.0; the high molecular weight segment is usually reported to have a slope of about 3.4.[12] Also within the context of this simplified picture of rheological behavior, M_c indicates a transition in the nature of the response of assemblies of polymer molecules to stress. Solutions and melts of (nonpolar) polymers in the lower molecular weight domain are Newtonian fluids and those in the higher molecular weight domain are markedly non-Newtonian.[15] Indeed viscosities of polymeric fluids with molecular weights one or two decades greater than M_c decrease by one or two orders of magnitude when they are subjected to shear rates of 10^2–10^3 sec^{-1}.

In addition, solutions and melts in the low molecular weight regime demonstrate zero-shear-rate viscosities in good agreement with the theory proposed by Debye and Bueche[12–14,16,17] and there is substantial evidence that the Rouse theory gives a good quantitative description of their viscoelastic behavior.[6,8–11,18] Above M_c, however, the theories of Debye and Bueche and Rouse no longer apply. Since these theories assume that the polymer molecules act independently, it follows that above M_c cooperative motion between neighboring chain molecules is required for polymeric fluids to respond to applied stress. This type of cooperative chain motion is interpreted as chain entanglement, and it is also assumed that it is disentanglement[15,19] that is responsible for non-Newtonian behavior above M_c.

According to the Rouse theory,[1] linear viscoelastic behavior of polymer solutions and melts should be described by sums of Maxwell elements with spring constants equal to nkT and relaxation times τ_p given by

$$\tau_p = \sigma^2 N^2 f_0 / 6\pi^2 p^2 kT \qquad (1)$$

where n is the number of molecules per unit volume, kT is Boltzmann's constant times the absolute temperature, N is the number of statistical segments per chain, σ^2 is the mean-square distance between the two ends of a statistical segment, and the index p relates each relaxation time to one normal mode of chain backbone motion.

We will examine linear viscoelastic behavior in terms of log–log plots of loss modulus G'' as a function of frequency ω from the terminal zone through the transition zone.[20] In agreement with the Rouse theory,[6,11,18] unentangled polymer systems show a rather abrupt change in slope at $\omega = \tau_1^{-1}$ from a value of unity in the terminal zone (where $G'' = \omega\eta_0$) to a value of one-half in the transition zone. In contrast, however, entangled systems have a plateau between the transition and terminal zones.[20] It has often been assumed that entangled systems also obey the Rouse theory, but that they have their longest relaxation times extended to even longer times by chain entanglement and that it is this effect that causes the characteristic plateau.[20,21] The applicability of such a modified Rouse theory has been questioned, however, and with some justification. In order to test the validity of such a theory, linear viscoelasticity measurements must be made from the terminal zone to well within the transition zone on polymer systems of sufficiently narrow molecular weight distribution. The results of one such study were not consistent with the modified Rouse theory;[22] results of other experiments were not interpreted in detail in terms of molecular theory.[23] The goal of this work, therefore, was to find if linear viscoelastic behavior of concentrated solutions of polymers of narrow molecular weight distribution could be adequately interpreted in terms of the Rouse theory by adjusting only the longest few relaxation times.

Experimental Section

Dynamic Viscometer. A specially designed and constructed dynamic viscometer was used in this research. It consisted of a freely damped torsional pendulum driving the probe of a variety of thermostated cup-and-bob or cone-and-plate viscometers (see Figure 1). The torsion element, which was one of several steel rods, was fixed rigidly to an upper support and supplied the stored energy required to drive the inertial element and viscometer probe in small-angle damped harmonic oscillation. In order to perform an acceptable experiment, the proper viscometer geometry had to be chosen so that most of the damping was supplied by the fluid in the cup (or on the plate) and only small corrections were made for damping due to internal friction of the torsional rod; air damping was negligible for all cases. The pendulum and viscosity probe were held on their axis to within an estimated ±3 × 10^{-4} in. by a nitrogen bearing. The angle of deflection of the pendulum was

---

(2) J. G. Kirkwood and J. Riseman, *J. Chem. Phys.*, **16**, 565 (1948).

(3) P. J. Flory, "Principles of Polymer Chemistry," Cornell University Press, Ithaca, N. Y., 1953, Chapter 14.

(4) C. W. Pyun and M. Fixman, *J. Chem. Phys.*, **44**, 2107 (1966).

(5) B. H. Zimm, *ibid.*, **24**, 269 (1956).

(6) N. W. Tschoegl and J. D. Ferry, *Kolloid Z., Z. Polym.*, **189**, 37 (1963).

(7) G. Harrison, J. Lamb, and A. J. Matheson, *J. Phys. Chem.*, **68**, 1072 (1964).

(8) J. E. Frederick, N. W. Tschoegl, and J. D. Ferry, *ibid.*, **68**, 1974 (1964).

(9) J. E. Frederick and J. D. Ferry, *ibid.*, **69**, 346 (1965).

(10) J. D. Ferry, L. A. Holmes, J. Lamb, and A. J. Matheson, *ibid.*, **70**, 1685 (1966).

(11) R. S. Moore, H. J. McSkimin, C. Gieniewski, and P. Andreatch, Jr., *J. Chem. Phys.*, **47**, 3 (1967).

(12) G. C. Berry and T. G. Fox, *Fortschr. Hochpolym.-Forsch.*, **5**, 261 (1967–1968).

(13) F. Bueche and F. N. Kelly, *J. Polym. Sci.*, **45**, 267 (1960).

(14) T. G. Fox and V. R. Allen, *J. Chem. Phys.*, **41**, 344 (1964).

(15) R. S. Porter and J. F. Johnson, *Chem. Rev.*, **66**, 1 (1966).

(16) P. Debye and F. Bueche, *J. Chem. Phys.*, **20**, 1337 (1952).

(17) P. Debye, *ibid.*, **14**, 636 (1946).

(18) P. E. Rouse, Jr., and K. Sittel, *J. Appl. Phys.*, **24**, 680 (1953).

(19) W. W. Graessley, *J. Chem. Phys.*, **47**, 1942 (1967).

(20) For a more detailed discussion of phenomenological and molecular viscoelasticity, see J. D. Ferry, "Viscoelastic Properties of Polymers," Wiley, New York, N. Y., 1961.

(21) J. D. Ferry, R. F. Landel, and M. L. Williams, *J. Appl. Phys.*, **26**, 359 (1955).

(22) A. V. Tobolsky, J. J. Alkonis, and G. Akovali, *J. Chem. Phys.*, **42**, 723 (1965).

(23) S. Onogi, T. Masuda, and K. Kitagawa, *Macromolecules*, **3**, 109 (1970).

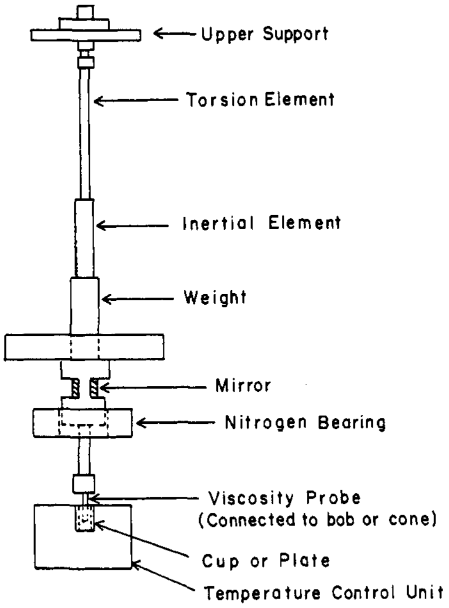

Figure 1. Freely-damped torsional pendulum dynamic viscometer.

monitored optically (see Figure 2). A collimated light beam was reflected from a mirror attached to the inertial element in an opening on the axis of the pendulum, and the reflected beam passed through a wedge-shaped slit and fell upon the sensing element of a phototube. After suitable amplification, the phototube produced a voltage proportional to the angle of deflection of the pendulum. The damped harmonic motion of the pendulum was then recorded with a Honeywell Visicorder.

By proper selection of cups-and-bobs or cones-and-plates, the instrument was capable of measuring dynamic viscosities between 10^{-1} and 10^{+6} P. The resonance frequency of the pendulum could be varied between 0.6 and 400 radians/sec by using a variety of torsion elements and weights on the inertial element. Nevertheless, the full range of frequencies could never be used for any given polymer solution without excessive changing of viscometer geometries. In any geometry, lowest frequencies were often overdamped for the most viscous solutions. Also, the highest frequencies required the largest torsion elements, and for the least viscous solutions the damping due to the internal friction of the elements often exceeded that of the solutions. For any given solution in any given viscometer geometry we were, however, able to obtain a minimum of 1.5 decades of frequency, which was sufficient for our purposes.

A more complete description of this equipment and its operation is given elsewhere.[24] The instrument was calibrated with various nonviscoelastic Newtonian oils, and loss moduli were determined from the experimental damped harmonic oscillations using recent analyses of freely damped viscoelastic systems.[25,26]

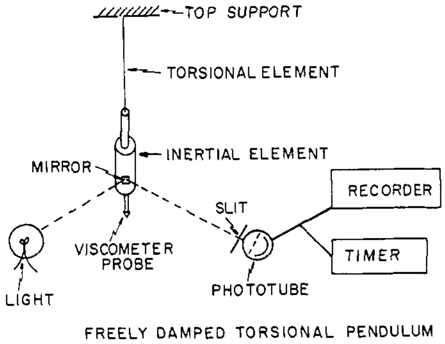

Figure 2. Instrumentation for dynamic viscometer.

Table I

Polymer Characterization

M_w	M_w/M_n
1.60×10^5	1.06
4.11×10^5	1.06
6.80×10^5	1.15

Solutions. Narrow molecular weight distribution polystyrene was purchased from Pressure Chemical Co., where it was synthesized using anionic techniques reported by Altares, Wyman, and Allan.[27] Each batch of polymer was statistically sampled and characterized by the manufacturer, and the results are listed in Table I. Di-2-ethyl hexyl phthalate (DOP) was used as solvent, primarily because of its extremely low vapor pressure, bp 232° (5 mm).

Solutions were made by weight to within ±0.01%. Solvent and polymer were weighed into the cone-shaped sample cup of a concentric cone mixer. Polymer and solvent were allowed to stay at 60° from 15 min to 2 hr. After the polymer had absorbed all the solvent, the cone-shaped rotor was placed in the cup. A nitrogen atmosphere was then introduced by passing the gas into the mixer through an inlet tube and allowing it to bubble out through a solvent seal. After 30 min of gentle purging the rotor was started. The sample was mixed at 12 rpm for between 48 and 72 hr, after which it was allowed to cool to room temperature. The semisolid sample was then removed and weighed to ensure that there was no appreciable change of weight. The total amount added to the mixer and the amount removed were never different by more than 0.4%. To check the uniformity of the solutions, samples of those made with the higher molecular weight polymers were taken from different parts of the mixer and their dynamic moduli measured at a given temperature and frequency. In each case the replicates agreed to within experimental error.

Even if we had been able to utilize conveniently the full range of frequencies available with the dynamic viscometer, we would not have been able to measure the entire spectrum of viscoelastic behavior from the terminal zone to well within the transition zone. But since the principle of time–temperature superposition is now well established,[20] this limitation offered no real difficulty. To simplify the experiments, therefore, each polymer solution was measured in only one cup-and-bob attachment. This restricted the frequency to about 1.5 decades at any given temperature. The dynamic viscosity of each solution was then measured at sufficiently close intervals of temperature between about 5 and 90° to affect good overlap of the G'' curves. From these temperature dependencies we then generated master curves of G'' as a function of frequency reduced to 25° that covered the entire desired range of frequencies. Shifting of the G'' curves in the nearly flat plateau zones was difficult for all the solutions, and indeed was impossible for the solution of polymer with 860,000 molecular weight. For that polymer the terminal zone had to be obtained from a zero-shear-rate viscosity measurement taken in a capillary viscometer.

Additional details on the instrument, calibration, and experimental procedure can be found elsewhere.[24]

Results and Discussion

Time–Temperature Superposition and Zero-Shear-Rate Viscosity. Compositions of the solutions that were studied are listed in Table II. Results for solution 1 were typical; log–log plots of G'' *vs.* ω at various temperatures for this system are shown in Figures 3 and 4. After time–temperature superposition, these data yielded the master curve reduced to 25° shown in Figure 5. We present only the master curves for solutions 2, 4, and 5, and they are found in Figures 6, 7, and 8. Only the transition zone was determined for solution 3, and therefore these results are not presented graphically.

---

(24) R. I. Wolkowicz, Ph.D. Thesis, University of Pennsylvania, 1968.

(25) W. C. Forsman, *Macromolecules*, **4**, 262 (1971).

(26) L. C. E. Struik, *Rheol. Acta*, **6**, 119 (1967).

(27) T. Altares, D. Wyman, and V. Allan, *J. Polym. Sci., Part A*, **3**, 221 (1964).

TABLE II

SOLUTION COMPOSITIONS WITH ASSOCIATED DETERMINED VALUES OF MONOMERIC FRICTION FACTORS, EFFECTIVE LOCAL VISCOSITIES, AND MOLECULAR WEIGHTS BETWEEN ENTANGLEMENT POINTS

Soln no.	Mol wt	C, wt fraction of polystyrene	$\zeta_0 \times 10^6$ monomeric friction factor, (dyn sec)/cm	η_e, effective local viscosity, P^a	M_e, mol wt between entanglement points (from longest relaxation time)	M_e, mol wt between entanglement points (estd from steady-flow viscosity)
1	4.11×10^5	0.225	0.26	3.3×10^{-1}	2.8×10^4	6.6×10^4
2	4.11×10^5	0.332	2.2	2.8	2.1×10^4	4.5×10^4
3	4.11×10^5	0.485	82	1.04×10^2		
4	1.60×10^5	0.332	2.2	2.8	2.0×10^4	4.5×10^4
5	8.60×10^5	0.332	2.2	2.8	2.6×10^4	4.5×10^4

^{a} Solvent viscosity = 0.58 P.

Shift factors for data taken in the terminal and plateau zones obeyed Arrhenius temperature dependence, whereas data taken in the transition zone were better described by the WLF equation.[20] Activation energies for the Arrhenius behavior were 6.2 kcal/mol for solution 1 and 5.2, 6.5, and 5.3 kcal/mol for solutions 2, 4, and 5. These results are well within the range of values reported for other concentrated polymer solutions at temperatures sufficiently above their glass transitions.[28-30] According to the Rouse theory, activation energies for the last three solutions should be equal. This conclusion follows from the facts that all of these solutions have the same (or very nearly the same) polymer concentration, and that the molecular weights are all sufficiently high that we should expect little or no effect of chain ends on the monomeric friction factor. We thus interpret the variations in activation energies as resulting from error in our time-temperature superposition.

For all the solutions studied, the transition zone occurred near room temperature at experimental frequencies. Extensive shifts were thus required to determine the terminal zones. Much of the shifted data were in the plateau zone, and as can be seen in Figures 6, 7, and 8, all the plateaus are quite flat. Indeed the rubbery plateau of solution 5 was so flat that shifting was impossible. But there was enough of this sample to independently determine a zero-shear-rate viscosity at 25° using methods described previously.[31] We thus used the limiting relationship

$$G'' = \mu\eta_0 \tag{2}$$

to fix the terminal zone for sample 5. Given the terminal zone, data in the plateau zone could be shifted with confidence. Unfortunately, there was not enough of samples 2 and 4 to independently set the transition zones. As a check on our superposition procedure, therefore, we made a log-log plot of η_0 *vs.* molecular weight using the limiting viscosities of solutions 2 and 4 as determined from their terminal zones and the viscosity of solution 5 which was measured directly. The results are shown in Figure 9. The slope of the straight line is 3.4, which is just as one would have expected according to recently published work on the viscosity of concentrated solutions of polystyrene (of narrow molecular weight distribution)

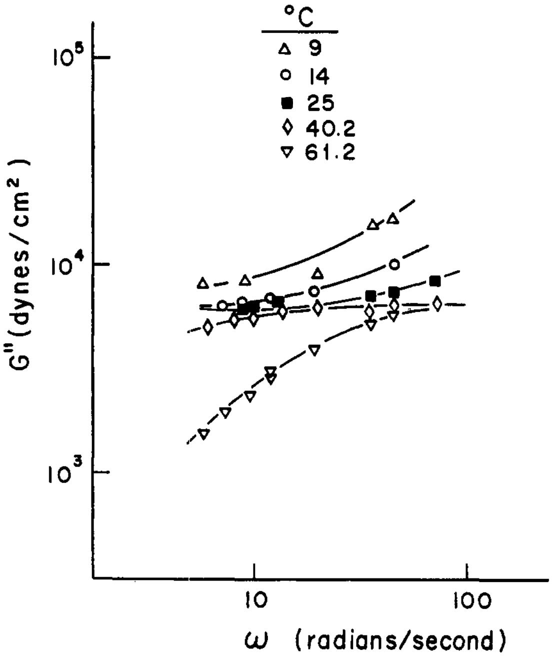

Figure 3. Loss modulus as a function of angular frequency at various temperatures for solution 1.

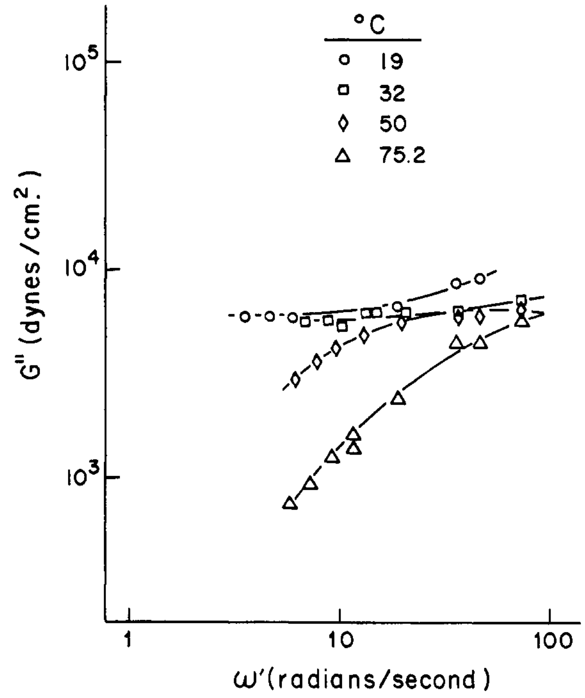

Figure 4. Loss modulus as a function of angular frequency at various temperatures for solution 1.

---

(28) M. Johnson, W. Evans, I. Jordan, and J. Ferry, *J. Colloid Sci.*, 7, 498 (1952).

(29) J. Ferry, E. Foster, G. Browning, and W. Sawyer, *ibid.*, 6, 377 (1951).

(30) J. Ferry, L. Grandine, and D. Udy, *ibid.*, 8, 529 (1953).

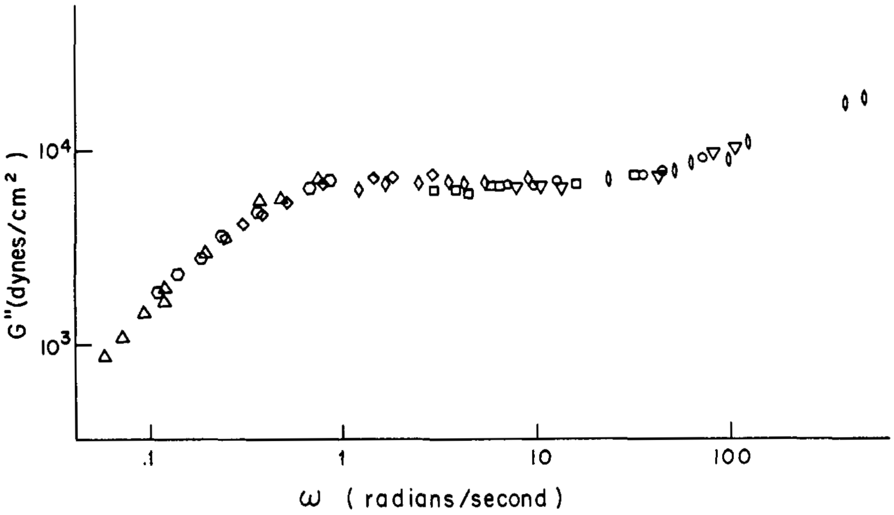

Figure 5. Master curve reduced to 25° for G'' as a function of ω for solution 1.

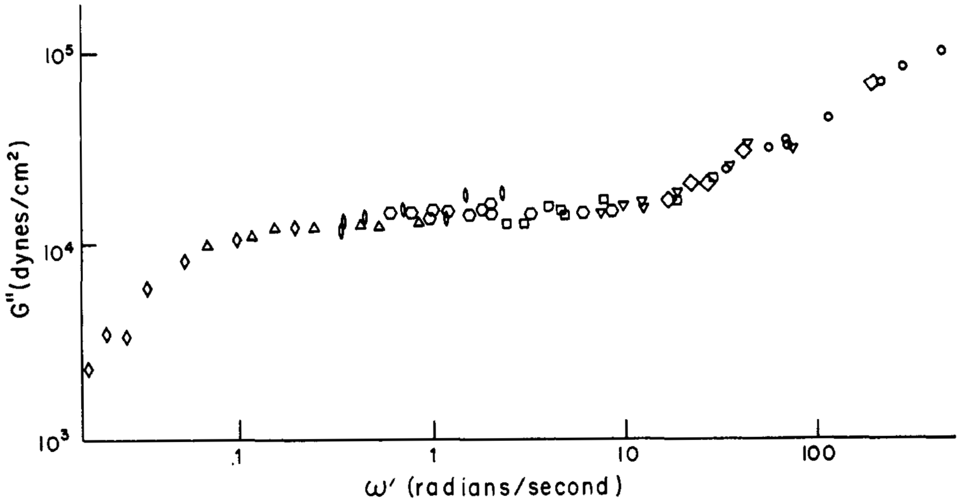

Figure 6. Master curve reduced to 25° for G'' as a function of ω for solution 2.

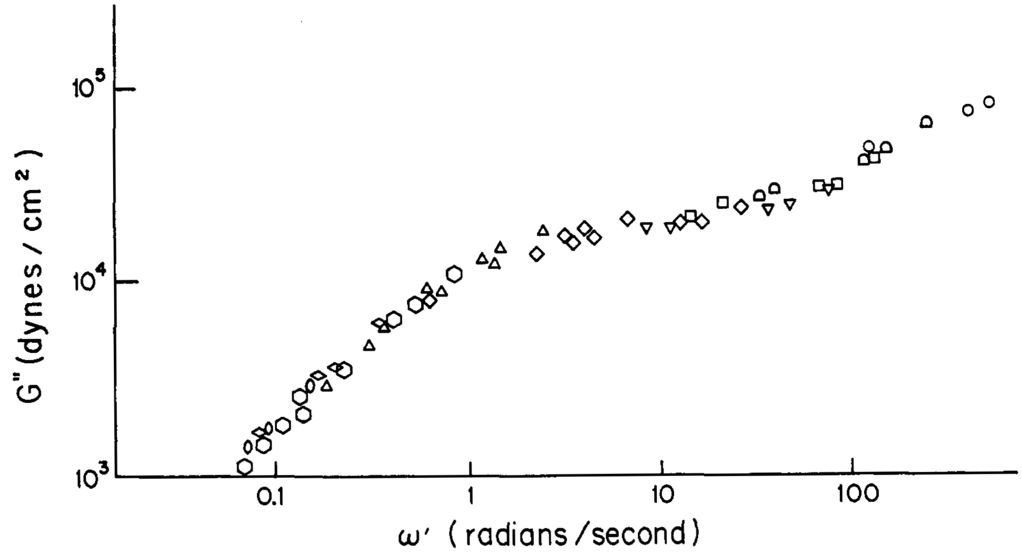

Figure 7. Master curve reduced to 25° for G'' as a function of ω for solution 4.

in the same solvent.[31] Clearly, then, our time–termperature superpositions yielded essentially correct master curves, but nevertheless master curves with sufficient error to account for the scatter in activation energies.

Monomeric Friction Factor and Effective Local Viscosity. The monomeric friction factor ζ_0 is defined as the drag coefficient of one statistical segment, f_0, divided by the number of repeat units per statistical segment, and its values can be calculated from the distribution of relaxation times in the transition zone.[20] In this work, however, we used the second-order

---

(31) D. Gupta and W. C. Forsman, *Macromolecules*, 2, 304 (1969).

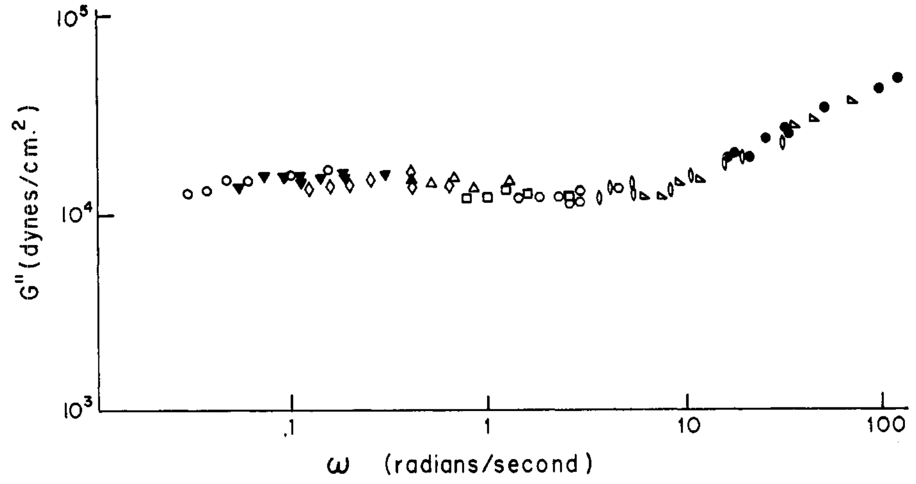

Figure 8. Master curve reduced to 25° for G'' as a function of ω for solution 5.

approximation of Staverman and Schwarzl[20] to eliminate the distribution of relaxation times in terms of G''. The result is

$$\zeta_0 = \frac{(G''M_0)^2 96}{\omega kT(a\rho N_0)^2} \tag{3}$$

where M_0 is the molecular weight of a repeat unit, a is the effective root-mean-square end-to-end distance of one repeat unit (and is defined as σ divided by the square root of the number of repeat units per statistical segment), ρ is the concentration of polymer in grams per cubic centimeter, and N_0 is Avogadro's number. We took a to be equal to 7.4×10^{-8} cm, which is its value calculated from the dimensions of polystyrene chains in a θ solvent.[20] Since the specific gravities of solvent and polymer were 0.99 and 1.05, respectively, we assumed a value of 1.00 for the specific gravity of all the solutions (making ρ and the weight fraction of polymer C numerically equal). The calculated values of ζ_0 are given in Table II.

A reasonable test of the Rouse theory is to find whether or not the experimentally determined monomeric friction factors are consistent with the local viscosity retarding the motion of a repeat unit. In order to make such a test, we assume that a repeat unit acts to a first approximation as a sphere with an effective radius r. Thus according to Stokes' law

$$\eta_e = (\zeta_0/6\pi r) \tag{4}$$

where η_e is the effective viscosity experienced by the repeat unit. Using 4.2×10^{-8} cm as the effective diameter of a styrene unit,[32] we obtain the effective local viscosities listed in Table II.

The local viscosity (just as ζ_0) increases rapidly with concentration due to the decrease in free volume available to any one repeat unit with the increasing presence of other polymer segments.

A plot of log η_e as a function of weight fraction polymer is shown in Figure 10. The straight-line portion of the curve has a slope of 18.8, which is in good agreement with the reported behavior of solutions of poly(n-butyl methacrylate) in diethyl phthalate.[33]

For the lowest polymer concentration (0.225 weight fraction) η_e is approximately equal to the viscosity of the solvent—indeed slightly lower. Clearly then, approximately 0.2 weight fraction polymer must be the cutoff point below which there is no effect of polymer concentration on local viscosity. Unfortunately, equipment limitations prevented us from going to lower concentrations to see if indeed the cutoff existed. Until the results of such measurements are available we tentatively conclude, just as in the study of concentrated solutions of poly(n-butyl methacrylate) by Ferry and coworkers,[33] that the values of effective local viscosity predicted by the Rouse theory are consistent with established notions of molecular mobility at the small-molecule level.

Experimental Relaxation Times. We assume that the Rouse theory, when appropriately modified to include the effects of chain entanglement, correctly describes the linear viscoelastic behavior of the polymer solutions studied in this research. To determine the experimental relaxation times, therefore, we first set the Maxwell model "spring constants" for each solution equal to nkT, which is equal to CRT/M. We then selected the set of relaxation times that best replicated

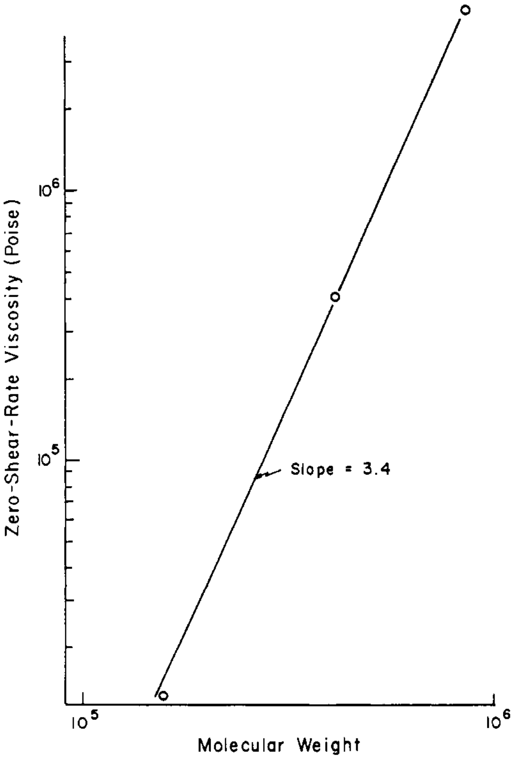

Figure 9. Viscosity as a function of molecular weight for solutions of 0.332 weight fraction polymer at 25°.

---

(32) C. Noller, "Chemistry of Organic Compounds," W. B. Saunders Co., Philadelphia, Pa., 1957, p 419.

(33) P. Saunders, D. Stern, S. Kurath, C. Sakoonkim, and J. Ferry, *J. Colloid Sci.*, **14**, 222 (1959).

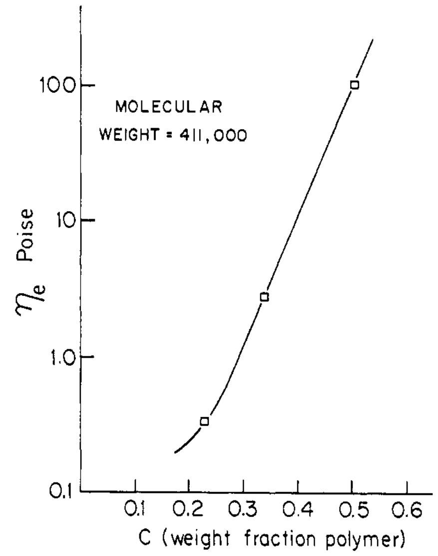

Figure 10. Effective local viscosity associated with one repeat unit as a function of weight fraction polymer.

each master curve of log G'' *vs.* log ω from the terminal zone through the low-frequency edge of the transition zone. The relaxation times were too close together in the transition zone to allow any curve fitting in that region. But this was of no consequence, since in the transition zone the relaxation times must decrease as p^{-2} with increasing p to effect the observed $^1/_2$ slope. By using this technique, we were able to reproduce the experimental master curves to within experimental error, which was about ±10%. The results of the curve fitting are given in Table III.

Clearly the relaxation times determined by such a method are somewhat arbitrary. The longest one or two could be determined easily to within ±10% by using the relation $\eta_0 = nkT\Sigma\tau_p$ as a check. But it was difficult to estimate the error in selecting the higher order values of τ_p. Repeated trails at fitting each curve indicated, however, that none of the experimental relaxation times could be varied by more than 15–20% without effecting serious deviation between experimental and theoretical curves. But in the next section we show that, for solution 1, experimental and theoretical relaxation times for $p = 2$ and 4 differ by a factor of about 2; so we conclude that the question of accuracy in the curve fitting procedure is still open for consideration. Nevertheless, we should like to point out that this procedure is not at all similar to curve fitting in the usual sense. The restriction imposed by setting the "spring constants" equal to nkT is a severe one, and certainly the correct higher order relaxation times must indeed fall near those determined graphically.

The Concept of Chain Entanglement. The idea of a molecular weight between entanglement points M_e is of central importance in the notion of chain entanglement. Not only is $2M_e$ interpreted as M_c, the break point in the log η–log M curve, but according to Ferry, Landel, and Williams,[20,21] it also defines $p_e = M/2M_e$, the critical entanglement index. They assume that ζ_0 for all normal modes of chain motion for which $p < p_e$ must be replaced by $Q_e\zeta_0$, where Q_e is the entanglement coupling factor, since these normal modes correspond to motion of lengths of chain of molecular weight greater than M_c. In order to be consistent with behavior in steady flow, it follows that

$$Q_e = 1 \qquad \text{if } p \geq p_e \tag{5a}$$

$$Q_e = (M/2M_e)^{2.4} \qquad \text{if } p \leq p_e \tag{5b}$$

TABLE III

EXPERIMENTALLY DETERMINED RELAXATION TIMES

Relaxation times, sec	Solution 4.11×10^5 [a] 0.332[b]	 4.11×10^5 [a] 0.225[b]	 1.60×10^5 [a] 0.332[b]
τ_a	1.84×10^1	1.11	3.1×10^{-1}
τ_b	1.67	7.1×10^{-2}	2.6×10^{-2}
τ_c	2.5×10^{-1}	7.1×10^{-3}	
τ_d	2.0×10^{-2}	1.3×10^{-3}	
τ_e		0.3×10^{-3}	

[a] *M*. [b] *C*.

As useful as the concept of the "molecular weight between entanglements" is, it is clearly an oversimplification. In a number of polymer systems that have been studied in some detail,[31,34] the plot of log η_0 *vs.* log M is not two intersecting straight line segments, but a smooth curve with a transition between straight line segments. From steady-flow measurements, then, we can identify a molecular weight range over which chains go from being completely unentangled to completely entangled with increasing chain length. And likewise, since the pth normal mode is associated with motion of lengths of chain of molecular weight (M/p), it is plausible that there would also be a range of values of p running from those associated with fully entangled normal modes to those associated with completely unentangled normal modes. In order to interpret the effect of entanglement on the various normal modes of chain motion, we thus replace Q_e by Q_p, an entanglement coupling factor which is a function of the index p. This new entanglement coupling factor is defined by

$$Q_p = \tau_p/\tau_{pR} \tag{6}$$

where τ_p is the pth relaxation time determined experimentally, and τ_{pR} is the value predicted by the Rouse theory and can be calculated from G'' in the transition zone. We can thus define three states of entanglement for normal modes of backbone motion: (1) fully entangled normal modes, all with equal values of Q_p (which must be proportional to $M^{2.4}$ to be consistent with observed viscosity–molecular weight relationships); (2) partially entangled normal modes, for which Q_p decreases rapidly with increasing p; and (3) unentangled normal modes, for which $Q_p = 1.0$.

Very likely the fact that we must consider a range of entangled chain lengths and partially entangled normal modes has contributed to the difficulty in reaching agreement on the value of M_e obtained from different experiments performed on the same system.[12,15] We find such an inconsistency within the results presented here. Although we do not have available η_0–M curves for $C = 0.225$ and 0.332, we can estimate the value of M_c at these concentrations from the reported viscosity measurements at $C = 0.30$ and 0.40.[31] For this system CM_c is a constant over the experimental range. We find, then, that for the two solutions of interest here

$$\text{when } C = 0.225 \qquad M_c = 1.33 \times 10^5$$

$$\text{when } C = 0.332 \qquad M_c = 0.90 \times 10^5$$

Values of M_e obtained from the above M_c values can be compared with those defined by the equation[20]

$$2M_e = MQ_e^{-(1/2.4)} \tag{7}$$

in which Q_e is given by

---

(34) M. M. Cross, *Polymer*, **11**, 238 (1970).

$$Q_e = \tau_1/\tau_{1R} \tag{8}$$

The comparison is given in Table II. Values of M_e calculated by the two different methods differ by approximately a factor of 2. This difference is not surprising considering the somewhat simplified notion of M_e.

Entanglements can also be interpreted as temporary crosslinks, and M_e can be calculated from the equation of rubber elasticity[20]

$$G_e = (RT/M_e)[1 - (2M_e/M)] \tag{9}$$

where G_e is the stress relaxation modulus in the rubbery plateau. We used the experimentally determined relaxation times to calculate $G(t)$ for solution 2, and its value in the plateau yielded a value of M_e of 6.6×10^4, which is about three times that calculated from the longest relaxation time. Data of Tobolsky, *et al.*, show a similar trend.[35] Their work with bulk polystyrene gave an M_e calculated from the $G(t)$ inflection of 3.4×10^4 which was three times the value that they calculated from the relaxation distribution.

In order to apply the notion of partial entanglement to the polystyrene solutions of interest here, we draw upon previously published viscosity–molecular weight relationships.[31] In these closely related solutions, we define the molecular weight range over which entanglement becomes fully developed as that range for which the smooth viscosity–molecular weight curve gives viscosities more than 10% greater than those predicted by the two intersecting straight lines. Since experimental error for these viscosities was ±10% or less, changes in entanglement effects are experimentally undetectable outside of this molecular weight range. For the solutions of 0.30 and 0.40 volume fraction polystyrene, these ranges are 0.5 and 0.8 decades centered about their respective values of M_c. We assume the 0.5 decade interval applies adequately to both the 0.332 and 0.225 weight fraction solutions, which implies that for these solutions entanglement effects become fully developed over the molecular weights from $(M_c/1.7)$ to $(1.7M_c)$.

Applying the above molecular weight intervals to the development of entanglements effects for the normal modes gives the following bounds on their degrees of entanglement.

$$\frac{M}{p} \geq 1.7M_c \qquad \text{fully entangled}$$

$$1.7M_c > \frac{M}{p} > \frac{M_c}{1.7} \qquad \text{partially entangled}$$

$$\frac{M}{p} \leq \frac{M_c}{1.7} \qquad \text{unentangled}$$

Before we can assign Q_p factors to the experimental relaxation times in Table III, we must identify the normal modes of motion that each is associated with. According to Ferry, Landel, and Williams,[21] we should make the assignments $\tau_1 = \tau_a$, $\tau_2 = \tau_b$, $\tau_3 = \tau_c$, etc. But according to recent theoretical work only odd-order normal modes can be affected by entanglements.[36] It could be possible, therefore, that some of the relaxation times listed in Table III are even-order ones that were unaffected by entanglement.

We have calculated Q_p values based on both the Ferry, Landel, and Williams (FLW) and Forsman–Grand (FG) theories.[36] In each case the relaxation times predicted by the Rouse theory were calculated from the equation

$$\tau_{pR} = (a^2M^2\zeta_0)(6\pi^2M_0{}^2p^2kT)^{-1} \tag{10}$$

using ζ_0 values calculated from the transition zone and values of the other parameters discussed previously. In Table IV, we list the Q_p values determined according to the FLW theory, and the results are plotted in Figure 11. In Table V and Figure 12 we present the Q_p values calculated according to the FG theory. Note in Table V that for the solution with 0.225 weight fraction polymer two experimental relaxation times fall close to those predicted by theory (for unentangled chains) for $p = 2$ and 4. Since, according to the FG theory, these two relaxation times should not have been affected by the presence of entanglements, the two experimental values were assumed to be those predicted by the Rouse theory and the deviations were assumed to be a consequence of an element of subjectiveness in curve fitting.

TABLE IV

FLW INTERPRETATION OF ENTANGLEMENT COUPLING FACTOR

	p	τ_p (Rouse), sec	τ_p (exptl), sec	Q_p
$M = 4.11 \times 10^5$	1	7.8×10^{-2}	18.5	2.4×10^2
$C = 0.332$	2	1.95×10^{-2}	1.67	95
	3	8.7×10^{-3}	2.5×10^{-1}	29
	4	4.9×10^{-3}	2.0×10^{-2}	4.1
$M = 4.11 \times 10^5$	1	9.3×10^{-3}	1.11	1.19×10^2
$C = 0.225$	2	2.2×10^{-3}	7.1×10^{-2}	31
	3	1.0×10^{-3}	7.1×10^{-3}	6.8
	4	5.8×10^{-4}	1.3×10^{-3}	2.7
	5	3.7×10^{-4}	0.3×10^{-3}	0.72
$M = 1.60 \times 10^5$	1	1.18×10^{-2}	3.1×10^{-1}	26
$C = 0.332$	2	3.0×10^{-3}	2.6×10^{-2}	8.8

Comparison of the correlations between Q_p and p (Figures 11 and 12) is insufficient to show which interpretation of entanglement is more correct. But examination of the number of entangled normal modes and their states of entanglement shows that our experimental results are consistent only with

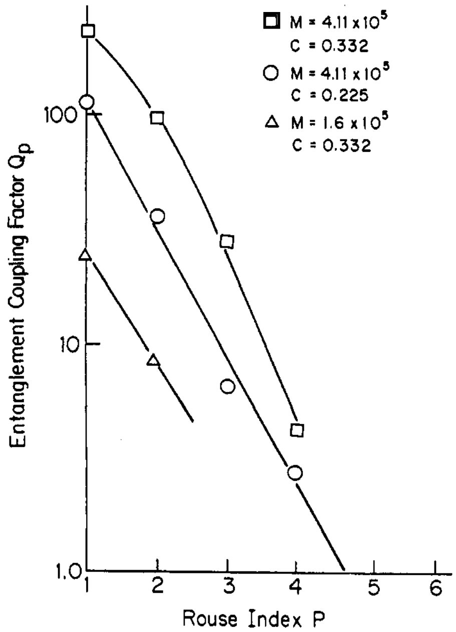

Figure 11. Entanglement coupling factor as a function of Rouse index according to the interpretation of Ferry, Landel, and Williams.

---

(35) A. Tobolsky, A. Mercurio, and K. Murakami, *J. Colloid Sci.*, 13, 196 (1958).

(36) H. S. Grand, Ph.D. Thesis, University of Pennsylvania, 1969.

Table V
Forsman–Grand Interpretation of Entanglement Coupling Factors

	p	τ_p (Rouse), sec	τ_p (exptl), sec	Q_p
$M = 4.11 \times 10^5$	1	7.8×10^{-2}	18.5	2.4×10^2
$C = 0.332$	2	1.95×10^{-2}		1.0
	3	8.7×10^{-3}	1.67	2.1×10^2
	4	4.9×10^{-3}		1.0
	5	3.1×10^{-3}	2.5×10^{-1}	80
	6	2.2×10^{-3}		1.0
	7	1.6×10^{-3}	2.0×10^{-2}	13
$M = 4.11 \times 10^5$	1	9.3×10^{-3}	1.11	1.19×10^2
$C = 0.225$	2	2.2×10^{-3}[a]	1.3×10^{-3} [a]	1.0 [a]
	3	1.0×10^{-3}	7.1×10^{-2}	71
	4	5.8×10^{-4}[a]	0.3×10^{-3} [a]	1.0 [a]
	5	3.7×10^{-4}	7.1×10^{-3}	19
$M = 1.60 \times 10^5$	1	1.18×10^{-2}	3.1×10^{-1}	26
$C = 0.332$	2	3.0×10^{-3}	3	1.0
	3	1.3×10^{-3}	2.6×10^{-2}	20

[a] These Rouse and experimental relaxation times should, in principle, be equal according to the Forshman–Grand interpretation

the assumption that odd-order normal modes alone are affected by entanglement. For the more dilute solution, Table VI indicates that five normal modes are associated with the motion of lengths of chain long enough to be entangled. Table IV and Figure 11 show that the FLW interpretation, which yields five entangled normal modes, is consistent with this. But in Table V and Figure 12, we see that the FG interpretation of the same data gives three entangled normal modes, which is also consistent with results shown in Table VI since the normal modes for $p = 2$ and 4 should be unaffected by entanglement.

Although it would seem that both interpretations of entanglement are consistent with the predicted and observed number of entangled normal modes, the dilemma is resolved by examining the state of entanglement predicted by each theory. If we assume the FLW theory to be correct, Table VI indicates there would be two fully entangled modes followed by three partially entangled ones. These predictions are inconsistent with the results shown in Table IV and Figure 11, which show values of Q_p that drop off rapidly with increasing p. If we interpret the data in Table VI according to the FG picture of entanglement, we should observe only one fully entangled normal mode followed by two partially entangled ones, which is consistent with the Q_p values given in Table V and Figure 12.

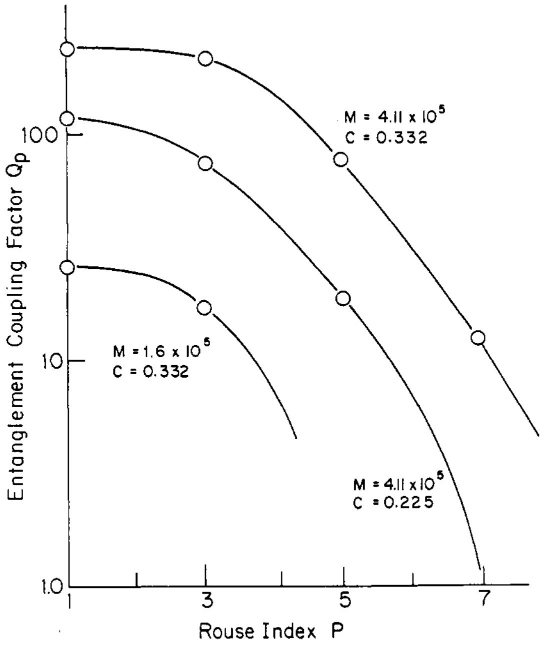

Figure 12. Entanglement coupling factor as a function of Rouse index according to the interpretation of Forsman and Grand.

Table VI
Degree of Entanglement of Various Normal Modes of Chain Motion in Solutions of 0.225 Volume Fraction Polystyrene ($M_c = 1.3 \times 10^5$)

p, Rouse index	$M \times 10^{-5}/p$	Deg of entanglement of normal mode
1	4.1	Fully entangled
2	2.1	Fully entangled
3	1.4	Partially entangled
4	1.0	Partially entangled
5	0.82	Partially entangled
6	0.69	Unentangled
7	0.59	Unentangled

Table VII
Degree of Entanglement of Various Normal Modes of Chain Motion in Solutions of 0.332 Volume Fraction Polystyrene ($M_c = 0.90 \times 10^5$)

$M \times 10^{-5}$	P, Rouse index	$M \times 10^{-5}/P$	Deg of entangelement of normal mode
1.60	1	1.60	Fully entangled
1.60	2	0.80	Partially entangled
1.60	3	0.53	Partially entangled
1.60	4	0.40	Unentangled
1.60	5	0.32	Unentangled
4.11	1	4.1	Fully entangled
4.11	2	2.1	Fully entangled
4.11	3	1.4	Fully entangled
4.11	4	1.0	Partially entangled
4.11	5	0.82	Partially entangled
4.11	5	0.69	Partially entangled
4.11	7	0.59	Partially entangled
4.11	8	0.51	Unentangled
4.11	9	0.46	Unentangled

For the more concentrated solutions, Table VII shows three and seven possible entangled normal modes for the lower and higher molecular weight polymers. The experimental results, however, give only two and four entangled modes. In addition, the Q_p values shown in Figure 12 decrease as is predicted in Table VII if we consider that only odd-order normal modes are affected by entanglement. Values of Q_p calculated on the assumption that all normal modes are effected by entanglements are inconsistent with the degrees of entanglement listed in Table VII.

In conclusion, the linear viscoelastic behavior of the polymer solutions studied in this work was consistent with the Rouse theory when it was modified to include the effects of chain entanglement. Best correlations were obtained by assuming that entanglements affect only those relaxation times associated with odd-order normal modes of chain motion.

Acknowledgment. This study was supported by the Advanced Research Projects Agency of the Department of Defense.